Annealing of Polypropylene/Poly(ethylene-co-Propylene) Blend. II. Influence of the Structure and Properties of Poly(ethylene-co-Propylene) and Blended Polyethylene on Impact Strength

JUNICHI ITO, KATSUO MITANI, and YUKIO MIZUTANI, *Fujisawa Research Laboratory, Tokuyama Soda Co., Ltd., 2051 Endo, Fujisawa City, Kanagawa 252, Japan*

Synopsis

The effect of annealing on the impact strength of PP/poly(ethylene-co-propylene) (PEP) and PP/PEP/PE blends was studied with regard to the structure of PEP and the polyethylene crystallinity. The tensile impact strength of annealed blends was remarkably affected by the PEP structure such as molecular weight and comonomer composition and the annealing temperature, while the brittle temperature was scarcely affected. For the PP/PEP/PE blends, annealing at temperatures above the melting point of PE lowers the tensile impact strength in a similar manner as the PP/crystalline PEP blend. These phenomena were explained on the basis of the deformation mechanism presented in the previous article, that is, a thicker interfacial layer of PP and PEP forms by means of annealing to increase the energy needed to deform the interface. By using a scanning electron microscope, the transition layer was observed at the interface between amorphous PEP and PE in the PP/amorphous PEP/PE blend after etching with nitric acid. The formation of a thicker transition layer between amorphous PEP and PE and a sizeable increase in PE particle size by annealing was observed. The phenomena should be correlated with the impact sensitivity, especially tensile impact strength, in the PP/crystalline PEP and PP/amorphous PEP/PE blends. A reasonable explanation of the microstructure in PP/PEP blends has been developed in terms of comonomer composition and melting property of PEP.

INTRODUCTION

Polypropylene (PP) has many such superior properties as rigidity, hardness, tensile strength, and heat resistance, but has some weak points on impact strength and low-temperature brittleness due to the high crystallinity and glass transition temperature (T_g) at around 0°C. To overcome such drawbacks, a number of modifications on polymerization and molding technique have been carried out. Many studies to improve the properties by means of polymer blending have also been tried because of the better simplicity. Among them, many attempts have been made by blending an elastomer to improve impact strength and low-temperature brittleness, which caused a considerable decrease in rigidity.[1,2] We found that annealing PP/elastomer blends improves their impact strength and low-temperature brittleness as well as rigidity.

In the previous paper,[3] the effect of annealing on the physical properties such as tensile impact strength (TIS), brittle temperature (T_b) and tensile strength of PP/amorphous poly(ethylene-co-propylene) (PEP) blends was

CCC 0021-8995/85/020497-17$04.00

studied to postulate a deformation mechanism. We suggested that the changes in dynamic properties of the annealed blends are caused by the presence of a thicker interfacial layer formed at the interface between two types of polymers and by the segregation of amorphous components out of the crystalline region of the PP matrix. It was also speculated that the structure of PEP might be an important factor in the formation of the interfacial layer.

The purpose of this work is to establish relationships between the impact properties and the structure of PEP in the annealed PP/PEP binary blends as well as to point out the interfacial layer which govern the impact properties. In particular, we are attempting to clarify the influence of such

TABLE I
Analysis of Polymers

(1) PP

Sample	MFI[a] (g/10 min)	$\overline{M}_w \times 10^{-4}$	$\overline{M}_w/\overline{M}_n$
PP-1	2.3	42.5	4.9
PP-2	4.5	28.1	4.8
PP-3	13	22.0	4.8

(2) PE

Sample	MFI[a] (g/10 min)	d	T_m (°C)
HDPE-1	0.70	0.957	131
HDPE-2	8.7	0.968	129
LDPE-1	10.7	0.922	115
LDPE-2	17.4	0.922	114

(3) PEP

Sample	MFI[a] (g/10 min)	EC[b] (mol %)	$\Delta H_{PE}/\Delta H_{PP}$[c] (cal/g)	T_m (°C)	T_g (°C)
PEP-1	0.58	80	0.1/0.0	115 /—	−41
PEP-2	0.74	78	0.0/0.0	—/—	−41
PEP-3	5.8	80	0.0/0.0	—/—	−38
PEP-4	0.23	68	5.8/0.4	124.5/146.5	−38
PEP-5	0.60	67	8.1/0.0	124.7/—	−38
PEP-6	1.8	66	8.1/0.0	124.6/—	−40
PEP-7	2.6	72	9.3/0.0	125.2/—	−45
PEP-8	4.4	69	8.2/0.0	125.8/—	−44
PEP-9	16	68	9.4/0.0	126.3/—	−42
PEP-10	5.0	30	2.1/2.3	121.8/146.7	−18
PEP-11	5.0	45	4.0/0.3	124.5/146.6	−27
PEP-12	1.3	85	16.9/0.0	125.8/—	−50

[a] Melt flow index (MFI) was measured at 230°C under 2.16 kg load according to ASTM-D 1238.

[b] Ethylene content.

[c] $\Delta H_{PE}/\Delta H_{PP}$ are the heat of fusion of PE and PP in a PEP, respectively, and the corresponding melting points are listed in T_m. PEP-1-3 and PEP-4-12 are termed amorphous PEP and crystalline PEP in the text, respectively.

compositional variables as molecular weight and comonomer composition of PEP and percentage of components in the blend on the annealed blend morphology. We are also investigating the effect of annealing conditions for PP/PEP/PE blend systems and the blend of PP and PEP with crystallizable ethylene segments on the impact properties.

EXPERIMENTAL

Polymers used in this study are listed in Table I with their characteristics. The characterizations were performed in the same ways as presented in the previous paper.[3] PP (Tokuyama Soda Co., Ltd.), high-density polyethylene (HDPE) (Mitsui Petrochemical Ind. Ltd.), low-density polyethylene (LDPE) (Sumitomo Chemical Co., Ltd.), and amorphous PEP (PEP-1 to PEP-3) (Mitsui Petrochemical Ind. Ltd.) were commercial grades.

The crystalline PEP (PEP-4 to PEP-12) was prepared by copolymerizing of ethylene and propylene by use of the catalytic system of $TiCl_3 \cdot 1/3$ $AlCl_3$ (Toho Titanium Co., Ltd.) and Et_2AlCl (Nippon Alminum Alkyls, Ltd.) described as follows.

The copolymerization was carried out at 60°C in 500 mL of dry n-heptane. A prescribed quantity (0.1–0.5 g) of $TiCl_3 \cdot 1/3$ $AlCl_3$ was added to a 1-L stainless-steel autoclave fitted with a stirrer under a argon stream. Propylene, ethylene, and hydrogen, the quantities of which were calculated from the monomer reactivity ratios ($r_1 = 0.24$, $r_2 = 41$), were successively introduced into the autoclave. The polymerization was started by injecting an amount of Et_2AlCl calculated to be $Al/Ti = 4$ mole ratio into the autoclave under the pressure of feeding the ethylene–propylene gas mixture. The monomer gas mixture, the monomer composition of which was the same as that of the expected PEP, was fed to keep an autoclave pressure in the range of 3–4 kg/cm^2 during the polymerization. After a few hours the polymerization was quenched by introducing 50 mL of isopropanol. The polymer produced was dried in $vacuo$ at 60°C after washing with a sufficient amount of methanol.

Blending, annealing, and measurement of TIS and T_b were carried out in same manner as described in the previous paper.[3]

The observation of morphology of bulk was tried by using the nitric acid etching technique since the fracture surface does not represent an actual morphology. The same samples used for TIS measurement were etched with nitric acid ($d = 1.38$ HNO_3) at 108°C for 2.5 h.[4] By analyzing ^{13}C-NMR spectra of the treated samples, it was confirmed that all of the amorphous PEP in the blend has been eliminated under this etching conditions. The surface skin layer of the etched sample was easily stripped in several 10 min after dipping in acetone. The morphology of bulk under the surface skin layer was observed as the morphology of blends by a scanning electron microscopy (SEM).

RESULTS AND DISCUSSION

Influence of Structure of PEP on Annealing Effect of Binary PP/PEP Blends

Figures 1(a) and (b) show the dependence of the apparent average diameter of PEP particles on the melt flow index (MFI) and the comonomer composition of PEP in the PP/crystalline PEP blends, respectively. The average section diameters were measured manually from SEM micrographs of the blends etched with nitric acid. To determine the true particle size, the apparent particle diameter must be mathematically treated by means of the stereology theory. Stereological analysis would require a specific probe (plane) to evaluate particle size. The etched surfaces are poor probes for analysis. However, for convenience, we took the apparent value obtained from the micrographs as the average particle diameter of PEP since we found no pertinent data on the particle size distribution of such system as PP/PEP blend for calculation of the true value.

According to Tokita's theory,[5] which deals with the equilibrium particle size of the dispersed phase when the rates of breaking down and coalescence are balanced, the equilibrium particle size R^* can be expressed approximately as follows:

$$R^* \doteq [12p\sigma\Phi_D/(\pi\eta\dot{\gamma})][1 + 4p\Phi_D E_{DK}/\pi\eta\dot{\gamma})] \qquad (1)$$

where p is the probability that a collision results in a coalescence, σ is the interfacial tension, Φ_D is the volume fraction of dispersed phase, η is the apparent viscosity of the composite, $\dot{\gamma}$ is the shear rate, and E_{DK} is the macroscopic bulk breaking energy. Equation (1) indicates that the equilibrium particle size R^* becomes small when η and $\dot{\gamma}$ become large and when p, E_{DK}, σ, and Φ_D become small. It was reported that the particle size of dispersed phase varies with the melt viscosity of the dispersed phase and the PP matrix.[6] Thus it can be presumed that the changes of PEP particle size shown in Figures 1(a) and (b) would result from the complications of the factors described above.
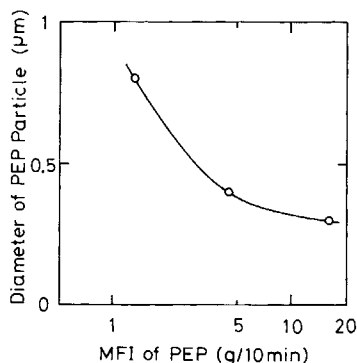

Fig. 1(a). Dependence of apparent average diameter of PEP particles on MFI of PEP used in PP-2/crystalline PEP (90/10) blend. Ethylene content of used PEP is 66–69 mol %.
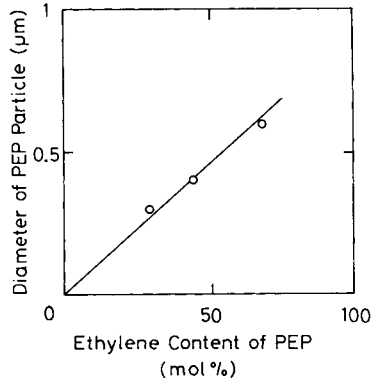
Fig. 1(b). Dependence of apparent average diameter of PEP particles on comonomer composition of PEP used in PP-2/crystalline PEP (90/10) blend. MFI of used PEP is 4.4–5.0 g/10 min.

Figure 2 shows the correlations of T_g and the heat of fusion of PE in a PEP (ΔH_{PE}) with the MFI of PEP, the ethylene content of which is 69 ± 3 mol %. Figure 2 depicts a decrease in MFI of PEP tends to shift T_g toward slightly higher temperature and to decrease the PE crystallinity in a PEP. The relationship between T_g and molecular weight may be interpreted with a widely used equation developed by Fox and Flory[7]:

$$T_g = T_{g,\infty} - K/M \qquad (2)$$

where T_g is the glass transition temperature for a liquid with a molecular weight M, $T_{g,\infty}$ is the glass transition temperature for a liquid with the infinite molecular weight, and K is a constant. The polyethylene crystallinity in a PEP having higher molecular weight may decrease on the basis of the mobility of polymer chain.

Figure 3(a) shows the variation of T_b of blends with the MFI of PEP at constant comonomer composition. The change in T_b (ΔT_b) by annealing is not controlled by the molecular weight of PEP, but is related to the improvement in T_b of the matrix PP, viz., $\Delta T_{bPP} = 29$–$16°C = 13°C \geq \Delta T_{b\,blend}$ by annealing at 140°C for 5 h. It has become apparent, therefore, that the
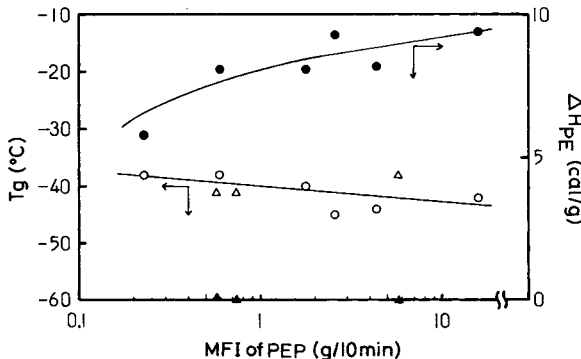

Fig. 2. Plots of ΔH_{PE} and T_g with MFI of PEP listed in Table I. ΔH_{PE}: (●) crystalline PEP; (▲) amorphous PEP. T_g (○) crystalline PEP; (△) amorphous PEP.
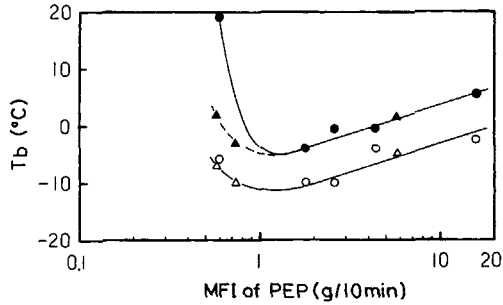
Fig. 3(a). Influence of T_b of binary PP-2/PEP (90/10) blends on MFI of PEP. Unannealed: (▲) PP-2/amorphous PEP (90/10) blends; (●) PP-2/crystalline PEP (90/10) blends. Annealed at 140°C for 5 h: (△) PP-2/amorphous PEP (90/10) blends; (○) PP-2/crystalline PEP (90/10) blends.

change in T_b by annealing in the binary PP/PEP blend is not influenced by the structure such as molecular weight, comonomer composition, and crystallinity of PEP.

Figure 3(b) shows the change of TIS of blends with the MFI and PEP at constant comonomer composition. TIS values of the unannealed blends with the amorphous PEP and the crystalline PEP change in the different manners in the region of the lower MFI of PEP than about 1 g/10 min, respectively, while those are plotted on the same line in the region of the higher MFI of PEP than about 1 g/10 min. TIS of the unannealed blends shows the maximum value at the MFI of 1 g/10 min as well as T_b. It is recognized in general that there appears to be an optimum size of the rubber particles for toughening in the rubber-modifier polymers. Impact strength will fall drastically if the diameter of the rubber particles is reduced below the critical values. There is some evidence for the rather loose fall in fracture resistance when the particle size is at diameters above the optimum. The critical particle size is not the same for all materials. It is reported
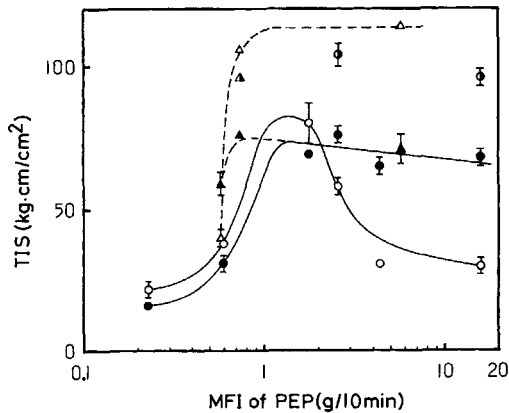

Fig. 3(b). Influence of TIS of binary PP-2/PEP(90/10) blends on MFI of PEP. Unannealed: (▲) PP-2/amorphous PEP (90/10) blends; (●) PP-2/crystalline PEP (90/10) blends. Annealed at 110°C for 5 h: (△) PP-2/amorphous PEP (90/10) blends; (◑) PP-2/crystalline PEP (90/10) blends. Annealed at 140°C for 5 h: (△) PP-2/amorphous PEP (90/10) blends; (○) PP-2/crystalline PEP (90/10) blends.

that the best estimated values are 0.8 μm for high-impact polystyrene, 0.4 μm for acrylonitrile–butadiene–styrene resin, and 0.2 μm for toughened poly(vinyl chloride).[8] From Figures 1(a) and 3, it is indicated that the optimum particle size on the impact strength in the unannealed PP/PEP blends seems to be about 1 μm for the applied polymers.

In contrast with T_b, TIS of the annealed blends is influenced by the structure of PEP as shown in Figure 3(b). TIS of the PP/amorphous PEP blends does not increase by the annealing at 140°C for 5 h below 0.7 g/10 min on the MFI of PEP used, but significantly improved under the same annealing condition above 0.7 g/10 min. It is interesting to note that TIS of the blend with amorphous PEP (MFI = 0.58) was decreased by annealing at 140°C. The reason could be ascribed to a poor dispersion of PEP in the PP matrix on the ground of the low MFI of PEP.

In contrast, TIS values of the PP/crystalline PEP blends in the high MFI region of PEP were decreased by annealing. All of the crystalline PEP used in this paper have polyethylene crystallinity but no polypropylene crystallinity. Such a crystallinity is due to a considerably different copolymerization reactivity between propylene and ethylene on the basis of the $TiCl_3$–Et_2AlCl catalyst used. TIS of PP/amorphous PEP having high MFI blends increased with the annealing temperature. On the other hand, the PP/crystalline PEP influence TIS on the annealing.

Figure 4(a) shows the effect of annealing on T_b of the binary PP-2/crystalline PEP blends in regard to the comonomer composition of PEP at constant MFI. As is well known, T_b of the unannealed PP/PEP blends is related to T_g of PEP,[9] which is shown in Figure 5. The effect of annealing on T_b for the comonomer composition of PEP is governed by the change of the annealed PP matrix in analogy with that on MFI of PEP in Figure 3(a), and is not scarcely affected by both of the crystallinity and the comonomer composition of the PEP used.

Figure 4(b) depicts the effect of annealing on TIS of the binary PP-2/crystalline PEP blends in regard to T_g of PEP as the case in T_b. The TIS value of the blend reaches maximum when the ethylene content in the
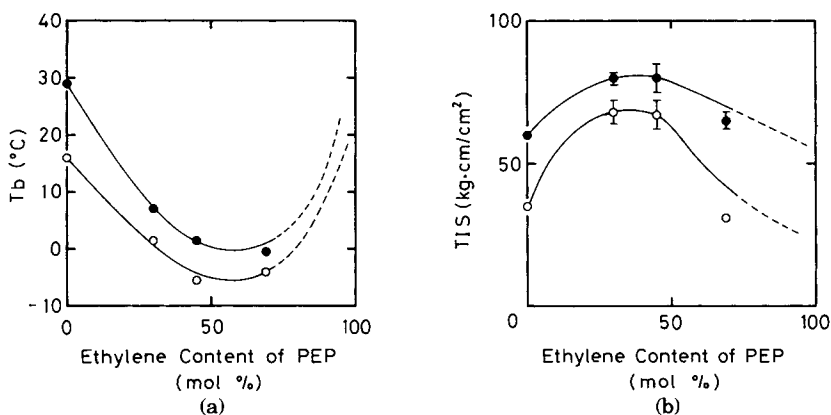

Fig. 4. Influence of impact strength of binary PP-2/crystalline PEP (90/10) blends on comonomer composition of PEP: (a) T_b; (b) TIS; (●) unannealed; (○) annealed at 140°C for 5 h. MFI of PEP are 4.4–5.0 g/10 min.
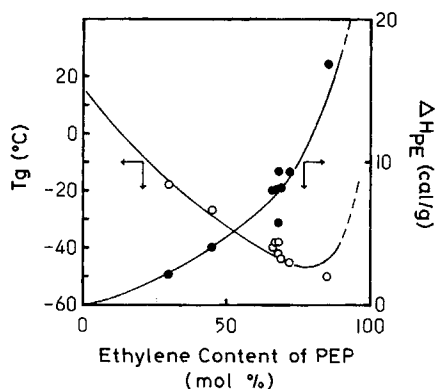
Fig. 5. Thermal properties of crystalline PEP listed in Table I on their comonomer compositions: (●) ΔH_{PE}; (○) T_g.

blended PEP is about 40 mol %. According to Figure 1(b), the PEP particle size decreases with the ethylene content of the blended PEP having constant MFI because the compatibility of PEP with the PP matrix increases with the decreasing of ethylene content. The particle size formed in the blend of PP and crystalline PEP with 40 mol % ethylene content seems to be optimum for toughening.

In the blend system of PP and crystalline PEP shown in Figure 4, the optimum particle size of PEP is 0.4 μm for TIS and 0.6 μm for T_b. These values are appreciably lower than the optimum size (1 μm) in the blend system of PP and crystalline PEP having the ethylene content of about 70 mol %. Such a discrepancy on the optimum size could be due to the difference in the molecular weight of PEP. TIS of all blends in Figure 4(b) was decreased by annealing at 140°C. As already shown in Figure 3(b), the reduction of TIS by annealing could be the effect of MFI of PEP, which may be concerned with the polyethylene crystallinity.

After all, it has been found that the annealing does not strongly affect T_b but TIS of the binary blends used PEP having the different structure. According to the previous paper,[3] the increase in the thickness of the PP–PEP interface on annealing seems to be a main factor for the improvement of TIS. However, the effect of annealing observed in the PP/crystalline PEP blend appears to be more complex than the effect observed in the PP/amorphous PEP blend. It is noticeable that TIS of the PP/crystalline PEP blend drastically changes after the annealing below or above the melting point of the crystalline PEP.

The transition layer at the interface between PP and PEP will grow in the annealed PP/PEP blends. When the blend is annealed above the melting point of crystalline PEP, a part of amorphous PP will be rejected from the crystalline region. However, the growth of the transition layer in the PP/crystalline PEP blend must be hindered owing to the incompatibility of the amorphous PP rejected and the melting polyethylene segments of PEP. The crystallinity of PEP increases with MFI and ethylene content of PEP. Consequently, the degree of hindering the growth of the transition layer will increase.

The Effect of Annealing of the Ternary PP/PEP/PE Blend

In the binary PP/PEP blend, it was noticeable that the annealing at temperatures above the melting point of the crystalline PEP decreases TIS of the blend. In order to consider the behavior of the polyethylene in the crystalline PEP in more detail, the influence of polyethylene component on the annealing of the ternary PP/amorphous PEP/PE blend will hereinafter be discussed.

Table II shows the effect of annealing on TIS and T_b for the ternary blends, and Figure 6 depicts the melt behavior of PP-2, PEP-12, and HDPE-1 applied in Table II. The annealing at 110°C promotes their recrystallization. On the contrary, the annealing at 140°C completely melts PEP and PE dispersed in the solid PP matrix. The effect of annealing of PP and the PP/PEP blend is the same as described previously. The annealing of PP shows lower TIS but improves T_b with the increase of the annealing temperature. In spite of the polyethylene crystallinity of PEP, the annealing of the PP/crystalline PEP blend improves both TIS and T_b. The effect of annealing of the PP/PEP blends on T_b is almost identical with that of the annealed PP. The annealing for the ternary PP/PEP/HDPE (80/10/10) blends increases TIS at 110°C but decreases at 140°C to less than the value of the unannealed blends as the effect of annealing of the binary PP/crystalline PEP having high MFI blend. However, it has been quite unexpected that the annealing at 140°C of the ternary blend using the crystalline PEP decreases T_b to less than the value of the unannealed blend. Such experimental results may support our speculation that the polyethylene crystallinity in a PP/crystalline PEP blend contributes to the unexpected reduction of the impact strength, especially TIS, of the annealed blend.

Figure 7 shows the influence of the amount of HDPE-1 added to the binary PP-2/PEP-3 blend on the effect of annealing for TIS. By the annealing of the ternary blends at 110°C, TIS increased by the same increment in the range of 0–10 wt % of HDPE content. However, by the annealing at
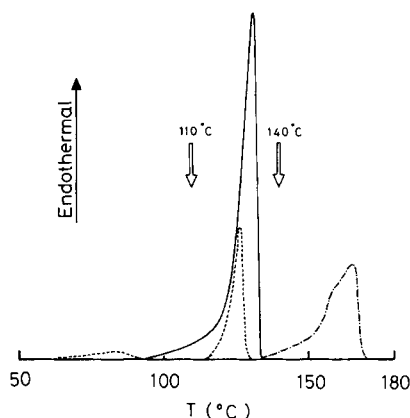

Fig. 6. DSC curves of polymers shown in Table II: (- · · · -) PP-2, $\Delta H = 20.4$ cal/g; (---) PEP-12, $\Delta H = 16.9$ cal/g; (———) HDPE-1, $\Delta H = 51.7$ cal/g.

TABLE II
Annealing Effect on Impact Strength of PP/PEP/HDPE Blends

PP/PEP/HDPE composition (wt %)			Unannealed		Annealed		
					110°C, 5 h	140°C, 5 h	
PP-2	PEP-2/PEP-12	HDPE-1	TIS (kg cm/cm²)	T_b (°C)	TIS (kg cm/cm²)	TIS (kg cm/cm²)	T_b (°C)
100	—/—	—	55 ± 4	29	44 ± 3	39 ± 1	16
90	10/—	—	72 ± 3	5	95 ± 4	107 ± 8	−1
90	—/10	—	76 ± 7	3	78 ± 4	116 ± 11	−7
90	—/—	10	55 ± 3	36	45 ± 3	23 ± 2	25
80	10/—	10	82 ± 5	−11	99 ± 11	14 ± 3	−9
80	—/10	10	87 ± 11	5	110 ± 1	35 ± 7	8
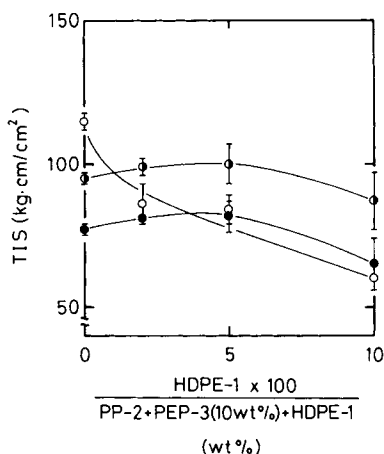
Fig. 7.   Influence of HDPE-1 added to binary PP-2/PEP-3 blend on effect of annealing for TIS: ($\bullet$) unannealed; ($\circleddash$) annealed at 110°C for 3 h; ($\circ$) annealed at 140°C for 3 h.

140°C, TIS tends to decrease with the addition of HDPE. These data also indicate that the PE component in a blend tends to decrease TIS when annealed above the melting point of PE.

A comparison of the polyethylene crystallinity of PP/crystalline PEP blend with that of PP/amorphous PEP/HDPE blend on the impact strength is particularly interesting. The binary PP-2/PEP-12 (90/10) blend in Table II has polyethylene crystallinity of 1.69 cal/g-blend since PEP-12 has the polyethylene crystallinity of 16.9 cal/g. The polyethylene crystallinity of 1.69 cal/g-blend in the binary blend corresponds to 3.3 wt % HDPE-1 in the ternary PP-2/PEP-3/HDPE-1 blend since HDPE-1 has the crystallinity of 51.7 cal/g. In Figure 7, TIS of the ternary PP-2/PEP-3/HDPE-1 (86.7/ 10/3.3) blend annealed at 140°C is almost equal to TIS of the unannealed blend. On the contrary, TIS of the PP-2/PEP-12 (90/10) blend annealed at 140°C in Table II is 40 kg · cm/cm² greater than the unannealed blend. This suggests that the behavior of a polyethylene crystalline fraction of PEP under annealing differs from that of the PP/amorphous PEP/PE blend; the crystallinity based on the molecular structure of PEP explicitly reflects the effect of annealing on TIS.

Figure 8 shows the influence of MFI of PE on TIS of the annealed binary PP-2/PE (90/10) blends. This experiment suggests that the reduction of TIS of the PP/PE blends by annealing does not relate to the molecular weight and the density of the blended PE but may depend upon the change of the crystalline structure of PP as a matrix or the interfacial adhesion.

Figure 9 depicts the influence of MFI of PE on TIS of the ternary PP-2/ PEP-3/PE blends annealed. The effect of annealing of the ternary blend containing PE having the lowest MFI is analogous to the tendency of the effect of annealing in Figures 3(b) and 7, that is, TIS decreases by annealing above the melting point of PE and increases by annealing under the temperature. And the effect of annealing at 110°C and 140°C of the ternary blend mixed with PE having high MFI except the lowest value is the same as shown in Figure 8. The PE component in the ternary blend containing PE having high MFI acts to decrease TIS by annealing even at 110°C. PE
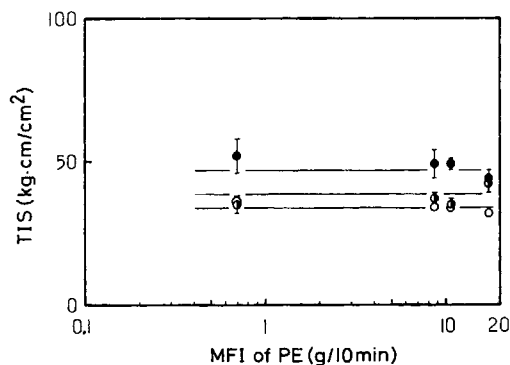
Fig. 8. Influence of MFI of PE on effect of annealing for TIS of binary PP-2/PE(90/10) blends: (●) unannealed; (◑) annealed at 110°C for 3 h; (○) annealed at 140°C for 3 h. All PE listed in Table I were used.

having MFI of 10.7 and 17.4 g/10 min are LDPE. Therefore, such specificity may be interpreted by the appreciable solubility or other interactions with ethylene sequences in PEP.

Morphology of Binary PP/HDPE and Ternary PP/Amorphous PEP/HDPE Blends

From some considerations of the effect of annealing on the impact strength of the binary and ternary blends, it has been concluded that the crystalline polyethylene component in the blend annealed above the melting point of PE reduces TIS but not T_b. The morphology of the HDPE in the annealed binary PP/HDPE and ternary PP/amorphous PEP/HDPE blends
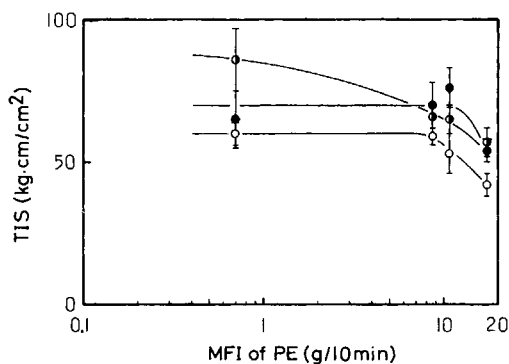

Fig. 9. Influence of MFI of PE on effect of annealing for TIS of ternary PP-2/PEP-3/PE(80/10/10) blends: (●) unannealed; (◑) annealed at 110°C for 3 h; (○) annealed at 140°C for 3 h. All PE listed in Table I were used.
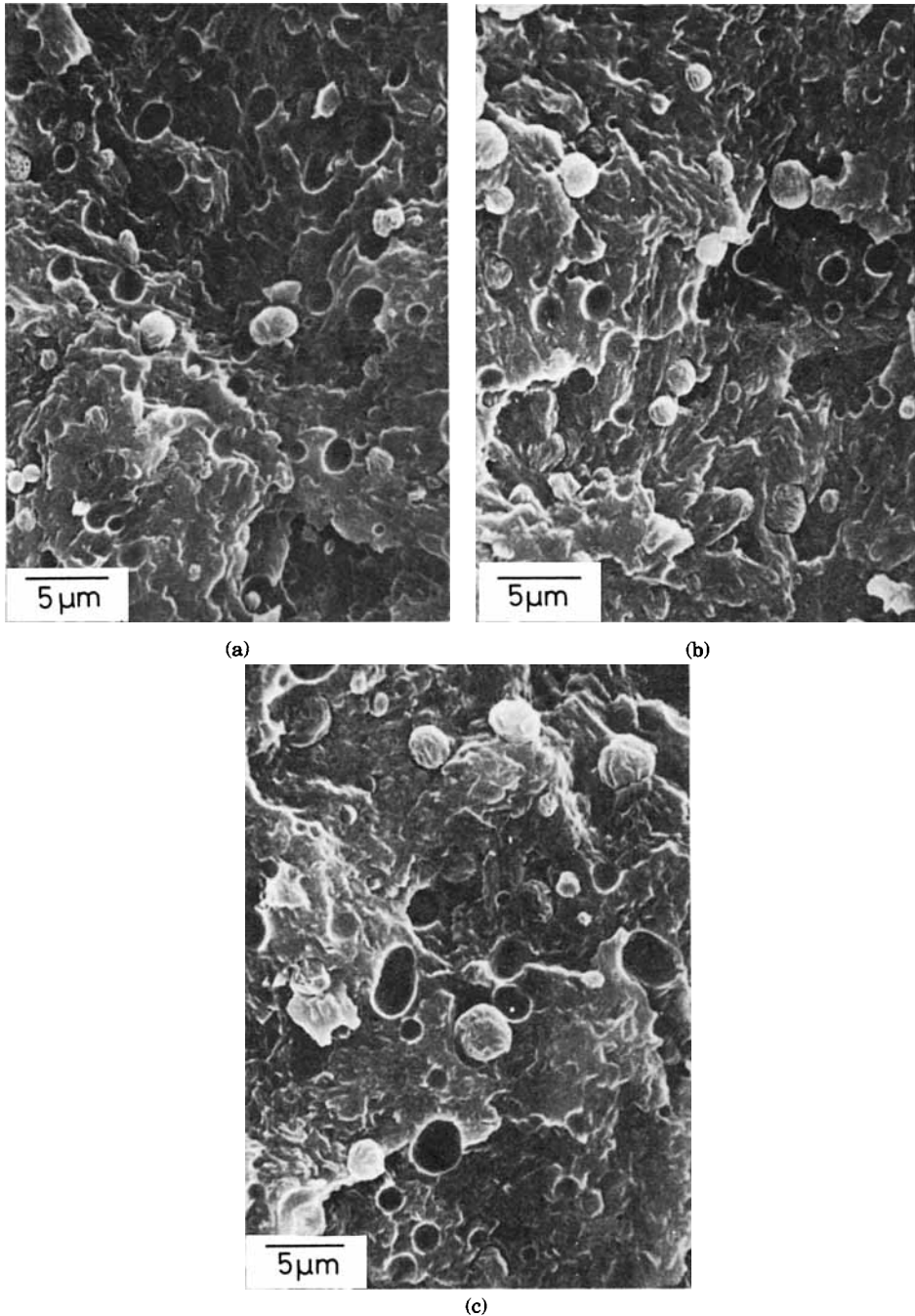
(a)

(b)

(c)

Fig. 10. SEM micrographs of binary PP-2/HDPE-1 (90/10) blend etched by nitric acid: (a) unannealed; (b) annealed at 110°C for 5 h; (c) annealing at 140°C for 5 h.

has been observed with SEM by employing the technique of nitric acid etching.

Figures 10(a)–(c) are the micrographs of the binary PP-2/HDPE-1(90/10) blend listed in Table II. It is apparent that particles are the HDPE phase

dispersed in the PP matrix. Any significant differences in the morphologies of the dispersed HDPE phase between the unannealed and annealed blends have been not recognized. These resulting morphologies seem to show that the change of the impact strength of the annealed PP-2/HDPE-1 blend depends upon the alternation of the crystalline structure of the PP matrix. Furthermore, the results in Table II suggest that the impact strength of the annealed PP-2/HDPE-1 blend may be also affected by the change in the interfacial adhesion or the recrystallization of PE filler as well.

Figures 11(a)–(d) show the micrographs of the ternary PP-2/PEP-2/HDPE-1(80/10/10) blend listed in Table II. The dispersed particles are apparently the HDPE phase because the condition of nitric acid etching to eliminate the amorphous PEP phase completely was applied for pretreatment of samples. In the ternary PP/PEP/PE blend system the PE phase may form a core in the dispersed PEP particle.[10-13] For the ternary blend system, such speculation that the HDPE phase and the PEP phase will form the core-shell structure in the PP matrix seems to be reasonable from the thermodynamic consideration. Namely, the surface tension of PP, amorphous PEP having ethylene content of 80 mol %, and PE are 22.6, 26.4, and 27.3 dyn/cm at 150°C, respectively, as reported by Hata and co-workers.[14] Each difference between those surface tension remains unchanged at such higher temperature, as 180°C under the roll mixing and 220°C under the compression molding, because the surface tension decreased in proportion to the increasing in the temperature according to the following equation:

$$\gamma = E^s - S^s T \tag{3}$$

where γ is the surface tension, E^s is the surface energy, S^s is the surface entropy, and T is the absolute temperature. S^s is about 0.06 erg/cm^2 · deg for PE. When PP, PEP, and PE are blended under the melting condition, the blend system will form the morphology to reduce the interfacial area and the interfacial energy thermodynamically.

In the unannealed and annealed ternary PP/amorphous PEP/HDPE blend, the sphere of the HDPE particle dispersed as the core in the PEP shell is not smooth but has many ridges. However, it should be noted that the morphology of the unannealed blend in Figure 11(a) may not suggest the morphology of the HDPE particle as the core in the true unannealed system because the sample had an additional thermal history of 108°C for 2.5 h during the nitric acid etching. Figures 11(a)–(c) suggest that the ridges over the particle surface will grow with increasing in the annealing temperature. Namely, the amorphous PEP shell may penetrate into the melt core of HDPE to form the transition layer by annealing.

Such variation in ridges on the HDPE particles as shown in Figures 11(a)–(d) supports that the polymer has an interpenetrating PEP–HDPE structure presented by Stehling and co-workers,[13] which may be called a transition layer. It grows up with the annealing temperature in the PP/amorphous PEP/HDPE blend.

We have calculated the thickness of the interfacial layer between two polymer phases with the aid of Helfand and Tagami's theory.[15] According

to the solubility parameters calculated by Hoy,[16] $|\delta_{PEP} - \delta_{PE}| = 0.04$ (cal/cc)$^{1/2}$ and $|\delta_{PP} - \delta_{PEP}| = 0.61$ (cal/cc)$^{1/2}$, where $\delta_{PP} = 7.38$, $\delta_{PEP} = 7.99$, and $\delta_{PE} = 8.03$ are solubility parameters of PP, PEP having ethylene content of 80 mol %, and PE, respectively. Therefore, assuming molecular weight of 10^5 for each polymer and temperature of 25°C, the thickness of the PEP–HDPE and PP–PEP interfaces before annealing are 300 and 20 Å, respectively. Although it is impossible to calculate each thickness after annealing since under the present conditions the temperature dependence of the energy interaction parameter or Flory's χ parameter is not revealed, each thickness is expected to increase with the annealing temperature.

Figure 11(a) shows that the average height of ridges on HDPE particles is 2000–3000 Å for the unannealed sample, but which has experienced the thermal history of 108°C for 2.5 h during the etching. The height increases to 7000–8000 Å for the sample annealed at 140°C for 5 h in Figure 11(c). If the ridges on the HDPE particles show the transition layer between HDPE and PEP, the thickness of the transition layer after annealing at 140°C is about 20 times larger than the thickness of the PEP–HDPE interface calculated above at 25°C.

Recently, evidences of cocrystallization to promote polymer miscibility have been reported on a blend of LDPE and PEP. However, even in those papers the cocrystallization of HDPE and PEP, in which EPDM was used as the PEP component, was considered to be almost impossible.[17,18] Therefore, it may be difficult to interpret such growth of ridges on HDPE particles in the ternary blend by annealing as shown in Figures 11(a)–(d) with the cocrystallization process.

As resulted in the previous paper,[3] TIS of a binary PP/amorphous PEP blend must certainly depend on the bonding strength of the PP–PEP interface. Also in the ternary PP/amorphous PEP/HDPE blend in this investigation, the impact deformation will occur at the interface between PP and PEP which includes the HDPE phase as the core. The above speculation seems to be supported on the basis of the SEM observation on the growth of the transition layer between PEP and HDPE and the comparison of the interfacial thickness of PP–PEP and PEP–HDPE as calculated above.

From Figures 11(a)–(d), the apparent average diameter of PEP particles including HDPE phase in the samples unannealed, annealed at 110°C for 5 h, annealed at 140°C for 5 h, and annealed at 140°C for 16 h are 2.2, 2.9, 3.3, and 3.3 μm, respectively. Namely, the PEP particles including HDPE phase are growing larger with the annealing temperature. The growth of PEP particles in the ternary blend annealed at 140°C appears to be complete by 5 h. On the other hand, the size of HDPE particles and the ridges on these also look like growing larger with the annealing temperature. And the particle size and the ridges of HDPE appears to be fized within 5 h in annealing at 140°C as well. The slight growth of HDPE particles is also observed in the annealed PP/HDPE blend, that is, from Figures 10(a)–(c) the apparent average diameter of HDPE particles unannealed, annealed at 110°C for 5 h, and annealed at 140°C for 5 h are 1.87, 1.94, and 2.2 μm, respectively. These phenomena of the particle growth by annealing suggest the migration or the rejection of the dispersed polymer in the annealed PP matrix.
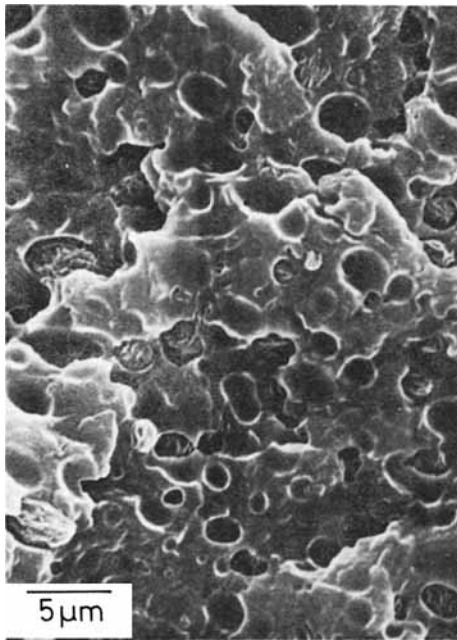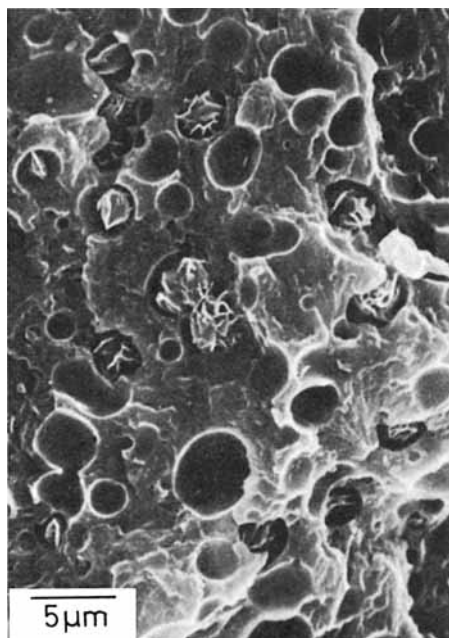
(a)
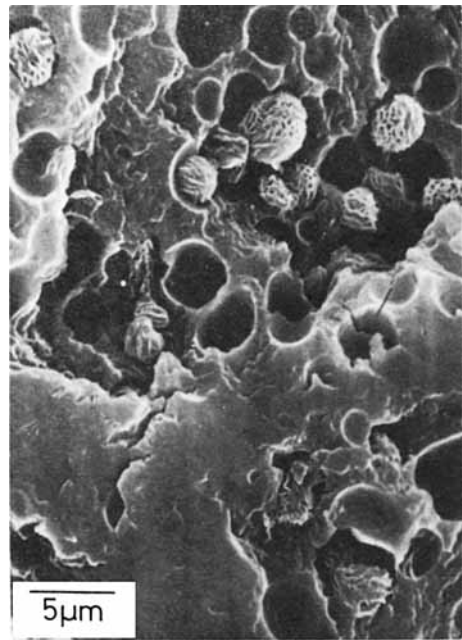
(b)
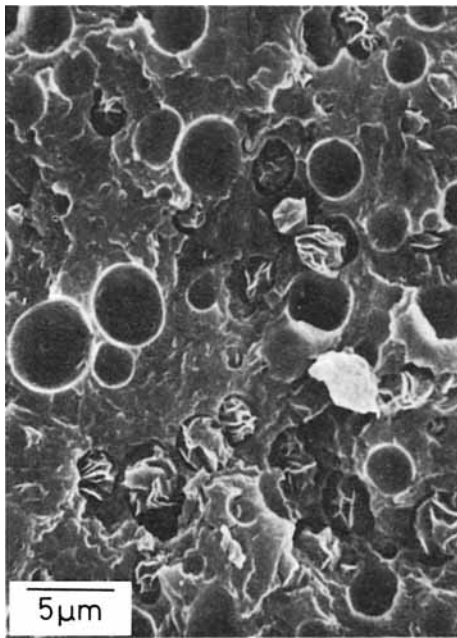
(c)

(d)

Fig. 11. SEM micrographs of ternary PP-2/PEP-2/HDPE-1 (80/10/10) blend etched by nitric acid: (a) unannealed; (b) annealed at 110°C for 5 h; (c) annealed at 140°C for 5 h; (d) annealed at 140°C for 16 h.

For the decrease in the impact strength, especially TIS, of the ternary blend annealed above the melting point of PE, the sizeable increase in PEP/HDPE particle size seems to be important. As mentioned before, the optimum particle size on the impact strength in the unannealed PP/PEP blend seems to be about 1 μm. By annealing, the thickness of PP–PEP interface and the size of dispersed particles will simultaneously grow larger with the treatment temperature. Therefore, the optimum particle size in annealed PP/PEP blend and annealed PP/PEP/HDPE blend will be larger than 1 μm. If the dispersed particle size reaches to the optimum value by annealing at about 110°C, the impact strength of the blends will be improved by annealing. Then, the impact strength of the blends annealed at 140°C will be lower than that of the blends annealed at 110°C or unannealed. The decrease in TIS by annealing at 140°C in the binary PP/crystalline PEP blend system may be also considered as in the case of the PP/amorphous PEP/HDPE since the molecular structure of the polyethylene part in the crystalline PEP prepared in this study is similar to that of HDPE.

References

1. J. Karger-Kocsis and V. N. Kuleznev, *Polymer,* **23,** 699 (1982).

2. L. D'Orazio, R. Greco, C. Mancarella, E. Martuscelli, G. Ragosta, and C. Silvestre, *Polym. Eng. Sci.,* **22,** 536 (1982).

3. J. Ito, K. Mitani, and Y. Mizutani, *J. Appl. Polym. Sci.,* **29,** 75 (1984).

4. H. Awaya, Y. Eda, K. Mitani, and Y. Mizutani, *Kobunshi Ronbunshu,* **39,** 99 (1982).

5. N. Tokita, *Rubber Chem. Technol.,* **50,** 24 (1977).

6. J. Karger-Kocsis, A. Kallo, and V. N. Kuleznev, *Acta Polym.,* **32,** 581 (1981).

7. T. G. Fox and P. J. Flory, *J. Appl. Phys.,* **21,** 581 (1950).

8. C. B. Bucknall, *Polymer Blend,* Academic, New York, 1978, Chap. 14.

9. L. E. Nielsen, *Mechanical Properties of Polymers and Composites,* Dekker, New York, 1974, Chap. 5.

10. R. C. Thamm, *Rubber Chem. Technol.,* **50,** 24 (1977).

11. W. M. Speri and G. R. Patrick, *Polym. Eng. Sci.,* **15,** 668 (1975).

12. T. Kuroda, *Polym. Prepr.,* Jpn., **27,** 22 (1978).

13. F. C. Stehling, T. Huff, C. S. Speed, and G. Wissler, *J. Appl. Polym. Sci.,* **26,** 2693 (1981).

14. T. Kasemura, N. Yamashita, K. Suzuki, T. Kondo, and T. Hata, *Kobunshi Ronbunshu,* **35,** 263 (1978)

15. E. Helfand and Y. Tagami, *J. Polym. Sci. B,* **9,** 741 (1971).

16. K. L. Hoy, *J. Paint Technol.,* **42,** 76 (1970).

17. G. A. Lindsay, C. J. Singleton, C. J. Carman, and R. W. Smith, *Am. Chem. Soc., Polym. Prepr.,* **19,** 206 (1978).

18. H. W. Starkweather, Jr., *J. Appl. Polym. Sci.,* **25,** 139 (1980).